

THE “SUPERCritical PILE” GRB MODEL: AFTERGLOWS AND GRB, XRR, XRF UNIFICATION

Demosthenes Kazanas¹, Apostolos Mastichiadis², and Markos Georganopoulos^{1,3}

¹*Astrophysics Science Division, NASA/GSFC, Greenbelt, MD 20771*

²*Department of Astronomy, University of Athens, GR 15784, Athens, Greece*

³*Department of Physics, JCA, UMBC, 1000 Hilltop Circle, Baltimore, MD 21250*

ABSTRACT

We present the general notions and observational consequences of the “Supercritical Pile” GRB model; the fundamental feature of this model is a detailed process for the conversion of the energy stored in relativistic protons in the GRB Relativistic Blast Waves (RBW) into relativistic electrons and then into radiation. The conversion is effected through the $p\gamma \rightarrow pe^+e^-$ reaction, whose kinematic threshold is imprinted on the GRB spectra to provide a peak of their emitted luminosity at energy $E_p \sim 1$ MeV in the lab frame. We extend this model to include, in addition to the (quasi-)thermal relativistic post-shock protons an accelerated component of power law form. This component guarantees the production of e^+e^- -pairs even after the RBW has slowed down to the point that its (quasi-)thermal protons cannot fulfill the threshold of the above reaction. We suggest that this last condition marks the transition from the prompt to the afterglow GRB phase. We also discuss conditions under which this transition is accompanied by a significant drop in the flux and could thus account for several puzzling, recent observations. Finally, we indicate that the same mechanism applied to the late stages of the GRB evolution leads to a decrease in $E_p \propto \Gamma^2(t) \propto t^{-3/4}$, a feature amenable to future observational tests.

Key words: Gamma Ray Bursts; Afterglows.

1. INTRODUCTION

Despite the great progress in the GRB field with the launch of *CGRO* and the discovery of their afterglows by *BeppoSAX* [1] (a fact that allowed the determination of their redshifts and provided an unequivocal measure of their distance and luminosity), a detailed understanding of the physics involved is still lacking. Several major issues concerning the dynamics and radiative processes of these events remain, to say the least, opaque. While the models of the GRB afterglow emission are reasonably successful in providing the time evolution of their afterglow flux [2, 3], there is an entire host of issues which are

tacitly ignored while discussing and modeling the details of GRB emission. Some of these issues have been with us since the inception of the cosmological GRB models, while others are rather new, the outcome of the wealth of new observations, most prominently those by *Swift* and *HETE*.

We provide below a partial list of the most important (to our view) such open GRB issues.

- The nature of the GRB “inner engine”. It is widely believed that this has its origin to the collapse of a stellar core or the merging of two neutron stars (we will not be concerned with it in the rest of the paper).
- The dissipation of the RBW kinetic energy. This is converted efficiently into relativistic protons (1/2000th of it into electrons) of Lorentz factor (LF) $\sim \Gamma$ (Γ is the LF of the blast wave). However, the efficient conversion of the latter into radiation, needed to account for the observed GRB variability, is one of the least discussed or explored issues.
- The energy distribution of the prompt GRB phase, in particular the presence of a peak in the νF_ν spectra at $E_p \sim m_ec^2$ [4], [5].
- The differentiation between prompt and afterglow phases. What determines, besides detector sensitivity, the separation in and the transition from the prompt to the afterglow stages in a GRB?
- Is there a unification between GRB, XRR and XRF? The discovery of transients with timing properties similar to those of GRB but with smaller E_p values (XRR, XRF) and smaller isotropic luminosities, E_{iso} , raised the question of their relation to GRB and the a possible unification of all these phenomena.

2. THE “SUPERCritical PILE” MODEL

The model outlined in the present note has been conceived to resolve the second of the issues enumerated above, i.e. that of the dissipation of the energy stored

in the form of relativistic protons within the RBW of a GRB. The name of the model is of relevance: Its basic physics is a radiative-type instability which can convert the free energy of the relativistic proton plasma into relativistic e^+e^- pairs on time scales R/c (R is typical size of the plasma), under certain criticality conditions[6],[7]. The nickname of the model derives from the fact that the criticality conditions are identical to those of a supercritical nuclear pile, where the free energy of nuclear binding can be explosively released once these conditions are fulfilled.

2.1. The Thresholds

The instability of a relativistic proton plasma, in distinction with that of a nuclear pile, involves a two step process: (a) The production of e^+e^- -pairs by the $p\gamma \rightarrow pe^+e^-$ reaction. (b) The production of additional photons, through the synchrotron process, which can then serve as targets for the above reaction to produce more pairs etc., offering the possibility of a runaway. Item (a) entails a *kinematic* threshold, while the true criticality is related to item (b) which in turn entails a *dynamic* threshold.

Consider a spherical volume of size R , containing a relativistic proton plasma of *integral* spectrum $n_p(\gamma) = n_o\gamma^{-\beta}$ (γ being the proton Lorentz factor), along with an (infinitesimal) number of photons of energy ϵ (in units of m_ec^2); these photons can produce pairs via the $p\gamma \rightarrow pe^-e^+$ reaction, provided that the proton population extends to Lorentz factors $\gamma > \gamma_c$ such that $\gamma_c \epsilon \simeq 2$. In the presence of a magnetic field B , the pairs (of Lorentz factor also equal to γ_c) produce synchrotron photons of energy $\epsilon_s = b\gamma_c^2$ where $b = B/B_{cr}$ is the magnetic field in units of the critical one $B_{cr} = m_e^2c^3/(e\hbar) \simeq 4.4 \cdot 10^{13}$ G. For the reaction network to be *self-contained* the energies of the seed and synchrotron photons should be equal, yielding the *kinematic* threshold of the process i.e.

$$\gamma_c \epsilon_s = \gamma_c^3 b \simeq 2 \quad \text{or} \quad \gamma_c \gtrsim (2/b)^{1/3}. \quad (1)$$

The reaction network will be *self-sustained* if *at least one* of the synchrotron photons pair-produces before escaping the volume of the plasma. Since the number of photons produced by an electron of energy γ is $N_\gamma \simeq \gamma/b\gamma^2 = 1/b\gamma$, the *dynamic* threshold implies that the column density of the protons at energy γ_c should be greater than $1/N_\gamma$ or

$$n_o \gamma_c^{-\beta} \sigma_{p\gamma} R \gtrsim b\gamma \quad (2)$$

where $\sigma_{p\gamma}$ is the cross section of the $p\gamma \rightarrow e^+e^-$ reaction.

In the case of the RBW of a GRB, on which the majority of particles are relativistic with mean energy $\langle E \rangle \sim$

Γ , we can eschew the presence of an accelerated non-thermal relativistic population and consider only the “thermal” relativistic protons present behind the forward shock of the RBW. These can be considered as monoenergetic of energy $\gamma_c = \Gamma$ (or of a Maxwellian of similar mean energy) where Γ is the Lorentz factor of the RBW. The linear dimension of the plasma in this case should be considered to be the (comoving) width of the RBW Δ_{com} , while its density the comoving proton density n_{com} . However, since $\Delta_{com} \simeq R/\Gamma$ and $n_{com} \simeq n_o\Gamma$, $\Delta_{com}n_{com} \simeq Rn_o$; hence we can express the *dynamic* threshold in terms of the shock radius R and ambient density n_o as

$$n_o \sigma_{p\gamma} R \gtrsim b\gamma \quad \text{or} \quad n_o \sigma_{p\gamma} R \Gamma^2 \gtrsim 2. \quad (3)$$

with the kinetic threshold used in the last step above.

It was noticed in [8] that the constraints on the thresholds given above can be alleviated if a fraction of the synchrotron photons (which are only at a distance R/Γ^2 ahead of the RBW), can scatter in a “mirror”. Scattering allows the RBW to catch-up with these photons, whose energy upon reinterception by the RBW is now increased by a factor $4\Gamma^2$, so that now the synchrotron photons have an energy $\epsilon' = 4\Gamma^2 b\gamma_e^2$. The kinematic threshold then becomes $\gamma_c \epsilon'_s \gtrsim 2$ or

$$b\Gamma^2 \gamma_c^3 \gtrsim \frac{1}{2} \quad \text{or} \quad b\Gamma^5 \simeq \frac{1}{2} \quad \Gamma \gtrsim \left(\frac{1}{2b}\right)^{1/5} \quad (4)$$

with the last steps assuming that the protons and electrons of the relativistic post-shock plasma have Lorentz factors $\gamma_c \simeq \gamma_e \simeq \gamma_p \simeq \Gamma$.

The dynamic threshold condition remains the same, however when simplified using Eq. (4) leads to

$$n_o \sigma_{p\gamma} R \gtrsim b\gamma \quad \text{or} \quad n_o \sigma_{p\gamma} R \Gamma^4 \gtrsim 2. \quad (5)$$

a condition a lot easier to fulfill than that of Eq. (3).

2.2. The Spectra: Scaling Arguments

It is of interest to note that the fundamental radiative process of this model, namely the $p\gamma \rightarrow e^+e^-$ reaction, involves a threshold electron energy [Eqs. (1) or (4)]. This is an important fact because it implies the absence of electron injection at energies lower than γ_c and leads naturally to a peak in the νF_ν GRB spectra at an (unspecified as yet) energy E_p . The presence of this peak energy has been one of the landmark features of GRB spectra [4], [5] and the issue of why $E_p \sim m_ec^2$ has vexed scientists over the years.

The more recent discovery of transients with values of E_p smaller than those found by *BATSE* suggested that this may in fact be a selection effect with (perhaps) little importance. However, the relation between E_p and the isotropic emitted energy E_{iso} discovered by Amati et al. [12] suggests that the value of E_p is not random but it is tied to the physics of the burst and (as we content) to the conversion of its kinetic energy to radiation.

The specificity of the above model allows the qualitative computation of the resulting spectra in a rather straightforward fashion: The basic process for photon production is synchrotron radiation with corresponding energy at $\epsilon_s \simeq b\Gamma^2$. The photons that are scattered on the “mirror”, they have, upon their re-interception by the RBW, energy (on the RBW frame) $E \simeq b\Gamma^4$. These photons will then scatter: (a) elastically by “cold” electrons ($\gamma \sim 1$) of the RBW to preserve their energy at $\epsilon_1 \simeq b\Gamma^4$, (b) inelastically by “hot” ($\gamma \simeq \Gamma$) electrons to boost their energy to $\epsilon_2 \simeq b\Gamma^6$ (or rather to $\min(b\Gamma^6, \Gamma)$ as the last scattering likely takes place in the Klein–Nishina regime). These energies will appear in the lab frame blue-shifted by a factor $\simeq \Gamma$ to occur correspondingly at energies $E_S \simeq b\Gamma^3$, $E_{BC} \simeq b\Gamma^5$, $E_{IC} \simeq \min(b\Gamma^7, \Gamma^2)$. If the process operates close to its kinematic threshold, then, by virtue of Eq. (4), the energy of the second (bulk Comptonized) component will be at $E_p \sim m_e c^2$, thereby resolving the issue raised by the *BATSE* systematics [4]. In addition to this aspect, this model also predicts the presence of additional peaks in the GRB spectra at energies $b\Gamma^3$ and $\min(\Gamma^2, b\Gamma^7)$ (all energies in units of $m_e c^2$). For typical values of Γ (~ 300), these are respectively $E_S \simeq 10$ eV and $E_{IC} \simeq 10 - 100$ GeV. The relative normalization of these three distinct components depends on the details of the processes involved [10] (also [9]) and imply the presence of prompt GRB emission in the optical and the *GLAST* energy bands.

2.3. Spectra and Variability: Detailed Calculations

The properties of the model outlined above have been explored in detail through numerical simulations. To this end the distribution functions of the protons, electrons and photons have been followed both in energy and time (or correspondingly in space), assuming a spherical shape for the emitting plasma. This approximation is justified by considering that the radial width of the RBW only $\Delta \simeq R/\Gamma^2$ in the lab frame, has a comoving frame size $\Delta_{\text{com}} \simeq R/\Gamma$; since an external observer “sees” only a fraction of the angular extent of the RBW of transverse spacial extent R/Γ (of the same size as the photon horizon), the radiating plasma on the comoving frame, can be considered as spherical of radius $r \sim R/\Gamma \simeq \Delta_{\text{com}}$. The calculations are thus preformed in the comoving frame and the radiation intensity is transformed to the lab frame at the very end.

The treatment (given in detail in [10]) follows closely that of Böttcher & Dermer [11] AGN variability study. One important feature of this treatment is the fact that the ra-

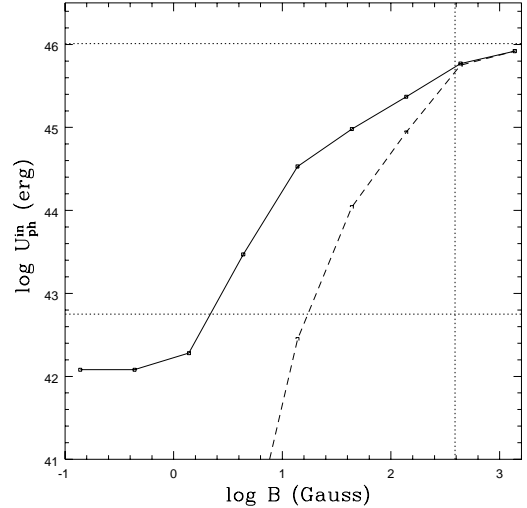


Figure 1. The total energy radiated by the protons in a case with $n_p = n_e = 10^4 \text{ cm}^{-3}$ as a function of the magnetic field strength B (both quantities measured in the comoving frame). The Lorentz factor of the RBW is $\Gamma = 400$. Solid and dashed lines represent the cases with and without relativistic electrons respectively. The lower horizontal dotted line is the total energy stored in electrons while the upper one is the energy stored in protons. The vertical dotted line is the equipartition magnetic field.

diation “reflected” in the “mirror” contributes to the proton and electron losses only after the RBW photons have scattered on the “mirror” and re-intercepted by the RBW. Therefore there is a causality constraint associated with the corresponding terms in these equations. Assuming the “mirror” to be extended, covering the range between R_{in} and R_{out} , these terms become effective only after time $t_c = (R_{\text{in}}/c) 2\beta_\Gamma/(1 + \beta_\Gamma)$ where β_Γ is the velocity of the RBW (normalized to c).

The calculations at this first stage were performed assuming a constant value for the RBW Lorentz factor Γ . These were performed under two different assumptions concerning the presence or not of relativistic electrons in the RBW, a feature crucial for the time development of the system: (a) No relativistic electrons initially present within the RBW. All necessary photons are produced (initially) from infinitesimal (numerical) fluctuations in the photon field. However, these suffice to produce pairs which in turn produce the required photons as discussed above (see fig. 5 of [10]). The increase in the ambient photons is exponential with characteristic time scale of the order of the light crossing time of the shock; as shown in the said figure, the characteristic time scale gets shorter the farther the parameters of system beyond their threshold values (i.e. the larger the value of the magnetic field B), with the process eventually saturating when enough pairs have accumulated to shield the protons from photon scattering. (b) Relativistic electrons are present in the RBW same in number and LF as the protons. These

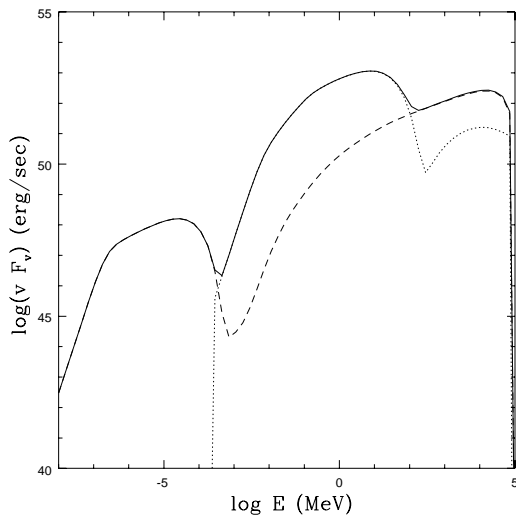


Figure 2. The GRB spectrum for a case of $n_p = n_e = 10^5 \text{ cm}^{-3}$ and $\Gamma = 400$ and $B = 25 \text{ G}$ at maximum flux. The three components discussed in the text are apparent with the middle one having a peak near 1 MeV.

cool very quickly to produce the photons necessary for the production of more electrons etc., as discussed above. The evolution in this case is much faster and the proton energy can be radiated away far more efficiently than in case (a) and for parameter values below those of the threshold.

These arguments are exemplified in Figure 1 where we plot the total energy radiated by the protons during the plasma traversal of a “mirror” of Thompson depth $\tau_{\text{mir}} = 1$, $R_{\text{in}} = 3 \cdot 10^{16} \text{ cm}$ and $R_{\text{out}} = 10^{17} \text{ cm}$. The presence of relativistic electrons facilitates the transfer of energy from the protons to the photons for a given value of B . For sufficiently large values of B , however, all the proton energy is eventually radiated away irrespective of the presence of the original relativistic electrons because the secondary pairs from the photon-proton collisions dominate the effects of the primary electrons.

At the same time, because of the presence of the additional photons due to the electron cooling, the maximum available luminosity can be achieved with parameter values (say that of the magnetic field B , below that necessitated by the threshold conditions.

In Figure 2 we also plot the resulting spectrum at flux maximum for a RBW with $\Gamma = 400$, $B = 25 \text{ G}$ and $n_p = n_e = 10^5 \text{ cm}^{-3}$ (the values of magnetic field and the density are measured on the RBW frame). The spectrum exhibits clearly the three components discussed in §2.2, with the middle one at an energy E_p of a few MeV. A decrease in the value of the magnetic field will result in a lower value of E_p , while a decrease in the proton density n_p (more correctly in the product $n_p \tau_{\text{mir}}$) will lead to a decrease in the luminosity of the bulk Comptonized component relative to those of synchrotron and Inverse

Compton ones.

3. THE AFTERGLOWS

3.1. A Definition for the Afterglow?

Following their discovery [1], afterglows have become an integral part of the the GRB study and, in fact, they presently consume the largest fraction of effort to understand the GRB phenomenon.

Based on the sparsely sampled early afterglow light curves and the ensuing theoretical models of their spectro-temporal behavior [2, 3], their light curves were expected to be smooth with rather well specified breaks in their time profiles and spectra. The launch of *Swift* and the possibility of continuously following a burst from the prompt to its afterglow stages, presented a number of surprises in variance with the earlier models; a partial list includes (a) the steep decline in X-ray flux shortly after (or perhaps in the transition to the afterglow from) the prompt GRB phase (b) an unexpectedly slow decline following this steep early phase and (c) the delayed large flares in the X-ray band [14] thousands of seconds since the beginning of the burst.

It appears, however, that in the excitement of the *Swift* results the issue of precise definitions for the prompt and afterglow GRB stages and the transition from one to the other has been neglected. In this respect, the “Supercritical Pile” model, precisely because it is founded on well defined and specific physical processes, does offer an answer to the previous question. The remaining issue, then, is to check whether this answer is in fact consistent with existing (or future) observations.

The kinematic threshold associated with the model (Eq. 4), in conjunction with the slowing down of the RBW as it accumulates mass from the surrounding medium, imply that the injection of electrons (and hence the GRB) should terminate as soon as Γ drops below the value that satisfies the kinematic threshold condition. However, in the presence of an accelerated population of relativistic protons that extends to energies much higher than $\Gamma m_p c^2$, i.e. the energy associated with the (quasi-)thermal post-shock population, the injection of relativistic electrons will continue even for $\Gamma \ll (2/b)^{1/5}$; this is because the non-thermal “tail” in the proton distribution guarantees the presence of protons with sufficiently high energies $\gamma_c \gg \Gamma$ which can fulfill the more general threshold condition $b \gamma_c^3 \Gamma^2 \gtrsim 2$.

Under these conditions the model predicts that electron injection will continue at a well defined energy but given in this case by the more general kinematic threshold of Eq. (1) rather than at $\gamma_e = \Gamma$. Herein we put forward the (*detector-sensitivity independent*) proposal that the transition from the prompt to the afterglow stage takes place when the RBW Lorentz factor drops below that of Eq. (4) or equivalently when $\Gamma < \gamma_c$.

Using the arguments presented in §2.1, one can now estimate the energies at which the spectral peaks discussed there will occur under these new circumstances. Because most of the GRB phenomenology covers the peak associated with the middle, bulk-Comptonized component we restrict ourselves to this component. Following the arguments presented earlier, this peak will now be (in the lab frame) at an energy

$$E_p \simeq b\gamma_c^2\Gamma(t)^3 \simeq 2 \left[\frac{\Gamma(t)}{\gamma_c} \right] < 1 \quad (6)$$

where the threshold condition $b\gamma_c^3\Gamma^2 \simeq 2$ has been used in the last step.

According to Eq. (6) above, the value of the peak energy of the νF_ν spectra is time dependent and presumably decreases with decreasing $\Gamma(t)$. The decrease in time can be determined once a relation between γ_c and Γ is found. Such a relation can be obtained from the threshold condition (Eq. 1) $b\gamma_c^3\Gamma^2 \gtrsim 2$ and it is $\gamma_c \simeq [2/b\Gamma(t)^2]^{1/3}$. For magnetic field in equipartition with the postshock plasma $b \simeq 10^{-14}n_o^{1/2}\Gamma(t)$, yielding $\gamma_c \simeq 6 \cdot 10^4 / [\Gamma(t)n_o^{1/6}]$, where n_o is the ambient (preshock) density in cm^{-3} . Finally, the relation between E_p and $\Gamma(t)$ reads

$$E_p \simeq 4.2 \cdot 10^{-2} n_o^{1/6} \left[\frac{\Gamma(t)}{50} \right]^2. \quad (7)$$

Therefore, one of the consequences of the electron injection process and spectrum formation within the present model is that the value of the energy of peak emission E_p should decrease with time as the GRB passes from the prompt emission to its afterglow stage. Eq. (7) provides a specific dependence of this energy on Γ and therefore on time. For the “standard” time dependence of Γ for RBW propagation through a medium of constant density ($\Gamma(t) \propto t^{-3/8}$) and for magnetic field in equipartition, $E_p(t) \propto t^{-3/4}$. Clearly the late time evolution favors observations by detectors which are more sensitive to lower energies, as indeed seems to be the case with the *Swift* observations.

3.2. Afterglow Light Curves

One of the surprising features of the GRB light curves obtained by *Swift* have been the steep decay of their X-ray flux, following the end of their prompt emission (or more specifically their becoming too faint for the BAT but not for the XRT). Generally, the models predicted flux decay $F_x \propto t^{-1}$ [2],[3], consistent with the observations of the earlier afterglows; steeper decrease in flux, attributed to emission from angles (between the fluid motion and the observer’s line of sight) $\theta > 1/\Gamma$ [13] were also considered leading to X-ray flux profiles $F_x \propto t^{-\alpha}$, $\alpha \gtrsim 2$.

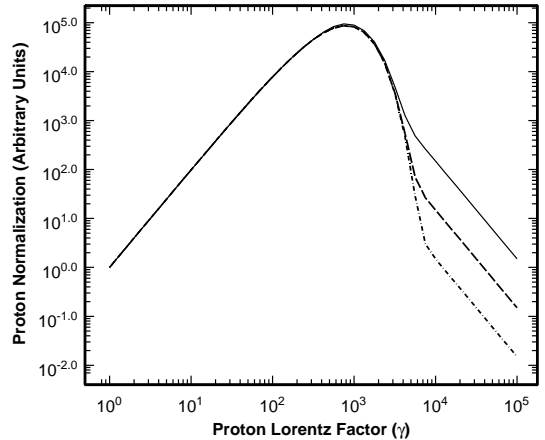


Figure 3. The proton Distribution Function used in producing the afterglow flux given in Figure 4. Besides a relativistic Maxwellian of the form $\gamma^2 e^{-\gamma/\Gamma}$ with $\Gamma = 400$, there is also a power law ‘tail’ to the spectrum with normalizations (relative to the peak of the Maxwellian) 0.1 (solid line), 0.01 (dashed line) and 0.001 (dot-dashed line).

However, the new observations exhibited decay rates as steep as t^{-6} [14], in clear disagreement with the theory.

The model we have presented here incorporates the possibility of producing such steeply falling light curves. The essence behind such behavior within the present model lies in the form of the proton distribution function behind the shock. Crucial for the extension of the model into the afterglow is the presence of a power-law “tail” in addition to the quasi-Maxwellian distribution of the bulk of the protons. Figure 3 shows the type of distribution we have been advocating in this section. We also assume that as the shock slows down the shape of the distribution function (i.e. the relative normalization of the power law and the Maxwellian) remains invariant and only shifts to lower energies. As the RBW slows down, the critical value of the proton energy necessary to fulfill the pair production threshold increases and as it sweeps past the maximum of the Maxwellian and into the power law section, the sharp drop in the proton density manifests as a sharp drop in the resulting photon flux. The corresponding change in the flux due to this effect is given in Figure 4, with the different curves representing the flux produced by the corresponding proton distribution of Figure 3. It is apparent that the model has sufficient freedom to account for this sort of observation.

4. GRB, XRR, XRF UNIFICATION?

The discovery of transients with E_p at energies smaller than those of the classic GRB [12] put in question the “characteristic” value of E_p indicated by [4] raised the

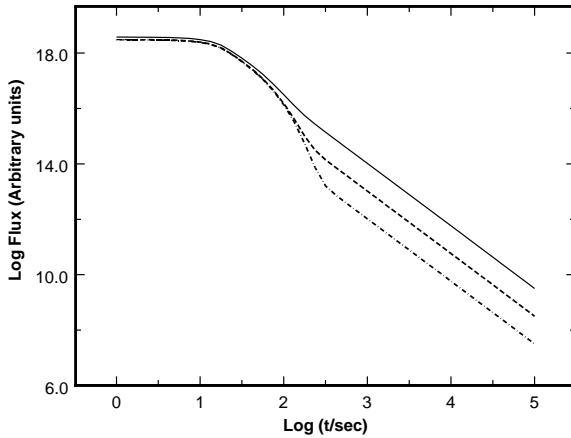


Figure 4. The synchrotron flux at energy $\epsilon = 10^{-6}$ as a function of time assuming $\Gamma(t) = \text{constant}$ for $t < 20$ seconds and $\Gamma(t) = (t/20)^{-3/8}$ for $t > 20$ seconds. The different curves correspond to the proton distributions with the power law normalizations given in Fig. 3. There is an apparent very steep drop of emission with time beginning at $t = 20$ sec.

issue of their nature and their relation to the “classic” GRB. This discovery and the restriction of the value of E_p within the “Supercritical Pile” model to range near the electron rest mass seemed to effectively rule out the specific model (and for that matter to any model that would produce a limited range in the value of E_p).

A resolution to this issue was suggested in [15], who proposed that the reduced value of E_p and the reduced peak flux of XRFs is related to the angle of the observer relative to that of the velocity of the RBW, with the XRFs being observed at large such angles. This (and any similar) interpretation, however, tacitly assumes the presence of a “unique” value for $E_p \simeq 1$ for a RBW moving along the observer’s line of sight, a feature that is not accounted for by the typical GRB model.

However, this particular account of the XRF - GRB unification has been challenged by the data of XRF 050416A [16]. The authors of this work pointed out that an orientation unification between the classic GRBs and XRFs implies that the source flux should increase as the RBW slows down since a larger fraction of the emitted luminosity would now be emitted into the observer’s line of sight. However, this particular event showed no such tendency, even though it was observed sufficiently early on so that this feature would not have been missed. Furthermore, it was shown that with an $E_p \simeq 15$ keV, it nicely filled the gap between GRB and XRF in the Amati relation [17].

The extension of the “Supercritical Pile” model with the additional consideration of the high energy proton “tail” suggested in the previous section can satisfy both these above constraints: For an initial RBW Lorentz factor smaller than that implied by the threshold condition of

Eq. (4), the production of pairs will take place by the interaction of the photons not with the protons of the Maxwellian part of the distribution but with the relativistic protons of its power law section. As indicated above, in this case, the value of E_p will be smaller than the electron rest mass the lower $\Gamma(t)$ lies below the threshold value necessary to pair produce with the protons of Lorentz factor Γ (i.e. those at the peak of the Maxwellian distribution). In fact, for field in equipartition with the protons, this value should be $E_p \simeq 1 n_o^{1/6} (\Gamma/250)^2$, so that for $\Gamma \lesssim 50$ this value will be in the range 20-40 keV, even for a RBW moving along the observer’s line of sight. Also, because of the smaller value of the RBW Lorentz factor Γ the total luminosity and radiated energy will be generally smaller, in agreement with the XRF observations.

5. THE “MIRROR”

One of the main aspects of the model described herein is that of the “mirror” whose purpose is to scatter the synchrotron photons so that they can be re-intercepted (blue-shifted now by $\sim 4\Gamma^2$) by the RBW. To this point it has been assumed that the albedo of this mirror is very close to 1, this being the reason that it does not figure in the expressions of the thresholds (Eqs. 4,3). It is easy to see that a smaller value for the mirror’s albedo will not change the kinematic threshold which is only concerned with the photon energies following the scattering by the mirror and the RBW. However, the dynamic threshold cares about the number of photons available to be scattered. Assuming that the fraction of the photons that scatter is proportional to the value of the “mirror’s” albedo τ_{mir} , then the corresponding expression for the dynamic threshold becomes

$$\tau_{\text{mir}} n_o \sigma_{p\gamma} R \Gamma^4 \gtrsim 1/2 \quad (8)$$

The issue of the nature of the “mirror” and the effect of its kinematic state on the thresholds has been discussed in detail in [10]. One can easily see that an outflowing “mirror” will lead to an increase in the value of the LF of the RBW Γ necessary to fulfill the kinematic threshold; however, the energy of the bulk Comptonized component of the resulting spectra will still appear, in the lab frame, at $E_{BC} \simeq 2m_e c^2$ (assuming that the process operates near threshold), thus preserving this feature of the model.

The simplest assumption concerning the “mirror” is that it is simply due to Thompson scattering on the electrons of the circumburst matter (it appears unlikely that any matter would not be fully ionized in the intense GRB photon field). In this case, $\tau_{\text{mir}} \simeq n_o \sigma_T R$, modifying the dynamic threshold to $\tau_T^2 \Gamma^4 \gtrsim (\sigma_T/2\sigma_{p\gamma})$, which for $n_o \simeq 10^3 \text{ cm}^{-3}$ and $R \simeq 310^{16} \text{ cm}$ yields $\Gamma \gtrsim 430$. These values of the density and radius are consistent with those encountered in a spherical wind of mass loss

$\dot{M} \simeq 3 \cdot 10^{-6} M_{\odot} \text{ yr}^{-1}$ and velocity $v \simeq 10^8 \text{ cm/s}$, parameters consistent with those associated with the Wolf-Rayet stars whose collapse presumably leads to a GRB.

The process responsible for producing the radiation observed in the *BATSE* and *Swift* energy bands within this model, i.e. the bulk Comptonization of the synchrotron radiation reflected in the “mirror”, provides the possibility of narrow ‘spikes’ in the GRB light curves, the presence of lags between hard and soft photons in these spikes and allows for rough estimates of these timing features: The synchrotron photons emitted by the RBW are at a distance $\Delta \sim R/\Gamma^2$ ahead of it and their scattering in the “mirror” produces (in the infinitely thin mirror approximation) a photon shell of width Δ ; the bulk Comptonized component is produced as these photons are swept by the RBW; this “sweeping” will take place on a time scale of order $\Delta t \sim \Delta/c\Gamma^2 \sim R/c\Gamma^4 \sim 10^{-4} \text{ sec}$ (and proportionally longer by $\delta R/\Delta$ if the “mirror” thickness δR is larger than Δ). Therefore, the model can produce fine structure in the GRB light curves by a process which could be considered as a variant of that of ‘internal shocks’, while in reality involving only external ones. In addition, photons arriving to the observer at slightly different paths after these repeated scatterings will have slightly different energies resulting to lags of the same order of magnitude, in general agreement with observations [18].

6. CONCLUSIONS

We have presented above the outline (and some details) of a model that provides a well defined procedure for converting the kinetic energy of the RBW of GRB into relativistic electrons and then into photons. To the best of our knowledge, this constitutes the first attempt to provide a detailed model of the dissipation (i.e. the conversion to radiation) of the kinetic energy of the GRB blast waves. In this respect the highly relativistic state of these flows is instrumental in effecting the dissipation of proton energy. Furthermore, the kinematic threshold of the reactions involved translates to a minimum energy in the injected electron distribution, which in turn leads naturally to a peak in the νF_{ν} GRB spectra that lies (because of the details of the same kinematics) in the vicinity of the electron rest mass, in agreement with observation.

The model provides also for a well defined demarcation between the prompt and the afterglow emissions based on the section of the proton distribution function which contributes to the electron injection: The prompt emission terminates when the injection shifts (because of the decrease in the RGW Lorentz factor) from the (relativistic) Maxwellian to the power law section of that distribution. The kinematics of the pair production and spectral formation then imply that the energy of peak emission E_p shifts to lower energies, also in general agreement with observation.

While our calculations to date have been limited to the

$p\gamma \rightarrow p e^- e^-$ reaction, the same photons could also produce pions, whose radiation can be added to the calculations, which become somewhat more complicated but without fundamental changes of the main point of the model. However, the possibility of photo-pion production can lead to a qualitatively new process, namely the production of neutrinos of energies that can be easily calculated: A rough estimate of the neutrino energy is $\sim 5\%$ the energy of the proton; given that the protons of the RBW frame have energies $E_p \sim \Gamma m_p c^2$ and in the lab frame $E_{p,\text{lab}} \sim \Gamma^2 m_p c^2$, the lab neutrino energy will be $E_{\nu} \sim 8 \text{ TeV} (\Gamma/400)^2$, a value of interest for the present and upcoming neutrino telescopes. One should note that this estimate does not consider the possibility of the power-law tail in the spectrum considered above. Should that be present, then correspondingly higher energies are possible.

Finally, this model can produce light curves with peaks of very narrow duration, despite the large size of the emission region, provided that the scattering medium has inhomogeneities of sufficiently short longitudinal dimensions. Robust as it is, this model cannot (as yet at least) address all questions pertaining to the physics of GRB, however, the GRB phenomenology is sufficiently diverse that addressing a fraction only of the open issues constitutes concrete progress.

ACKNOWLEDGMENTS

This work has been supported by the program Pythagoras at the University of Athens and an INTEGRAL GO grant at GSFC and UMBC.

REFERENCES

- [1] Costa, E. et al. 1997, *Nature*, 387, 783
- [2] Sari, R., Piran, T. & Narayan, R., 1998, *ApJ*, 497, L17
- [3] Sari, R., Piran, T. & Halpern, J. P. 1999, *ApJ*, 519, L17
- [4] Mallozzi, R. S. et al. 1995, *ApJ*, 454, 597
- [5] Preece, R. D. et al. 2000, *ApJS*, 126, 19
- [6] Kirk, J. G. & Mastichiadis, A., 1992, *Nature*, 360, 135
- [7] Mastichiadis, A., Kirk, J. G. A & A, 295, 613
- [8] Kazanas, D. & Mastichiadis, A., 1999, *ApJ*, 518, L17
- [9] Kazanas, D., Georganopoulos, M. & Mastichiadis, A. 2002, *ApJ*, 578, L15
- [10] Mastichiadis, A. & Kazanas, D. 2006, *ApJ*, 645, 416 (also *astro-ph/0512447*)
- [11] Böttcher, M. & Dermer, C. D. 1998, *ApJ*, 501, L51
- [12] Amati, F. et al. 2002, *A&A*, 390, 81
- [13] Kumar, P. & Panaiteescu, A. 2001, *ApJ*, 541, L51

- [14] O'Brien, P. T. et al. 2006, astro-ph/0605230
- [15] Ioka, K. & Nakamura, T. 2001, ApJ, 544, L163
- [16] Mangano, V. et al. 2006, ApJ (submitted), astro-ph/0603738
- [17] Sakamoto, T. et al. 2006, ApJ, 636, L73
- [18] Norris, J. P.; Marani, G. F.; Bonnell, J. T. 2000, ApJ, 534, 248